Electronic Supplementary Information

A simple and isothermal ligase-based amplification approach based on ligation-activated cleavage reaction

Fei Ma,‡ Huan Liu,‡ Chen-chen Li,‡ and Chun-yang Zhang*

College of Chemistry, Chemical Engineering and Materials Science, Collaborative Innovation Center of Functionalized Probes for Chemical Imaging in Universities of Shandong, Key Laboratory of Molecular and Nano Probes, Ministry of Education, Shandong Provincial Key Laboratory of Clean Production of Fine Chemicals, Shandong Normal University, Jinan 250014, China.

‡These authors contributed equally.

*To whom correspondence should be addressed. E-mail: cyzhang@sdnu.edu.cn; Tel.: +86 0531-86186033; Fax: +86 0531-82615258.

EXPERIMENTAL SECTION

Materials. All oligonucleotides (Table S1) were synthesized by Sangon Biotech Co., Ltd. (Shanghai, China). Duplex-specific nuclease (DSN) and 10× DSN reaction buffer (500 mM Tris-HCl, pH 8.0, 50 mM $MgCl_2$ and 10 mM DTT) were obtained from Evrogen Joint Stock Company (Moscow, Russia). T4 polynucleotide kinase (PNK), T4 RNA ligase 1 (Rnl1), T4 RNA ligase 2 (Rnl2), RNase If, and adenosine 5′-triphosphate (ATP) were obtained from New England Biolabs, Inc. (Ipswich, MA, USA). Diethylpyrocarbonate (DEPC)-treated water (RNase free) was obtained from TaKaRa Bio. Inc. (Dalian, China). Human cervical cancer cell line (HeLa cells) and lung cancer cell line (A549 cells) were purchased from Cell Bank of Chinese Academy of

Sciences (Shanghai, China). All other reagents were of analytical grade and used as received without further purification.

Table S1. Sequence of the Oligonucleotides[a]

note	sequence (5'-3')
donor RNA	GGU AAA GAU GG
phosphorylated donor RNA	G*G*U* A*A*A* G*A*U* G*G
acceptor RNA/RNA 1	UAA CAC UGU CU
phosphorylated acceptor RNA	U*A*A* C*A*C* U*G*U* C*U
Taqman probe	FAM-CCA TCT TTA CCA GAC AGT GTT A-Eclipse
RNA 2	PO_4-GGU AAA GAU GG
target DNA	CCA TCT TTA CCA GAC AGT GTT A
T-T	CCA TCT TTA CCT GAC AGT GTT A
T-C	CCA TCT TTA CCC GAC AGT GTT A
T-G	CCA TCT TTA CCG GAC AGT GTT A

[a] The asterisk indicates the phosphorothioate modification.

PNK Activity Assay. The detection of PNK involves three consecutive steps. Firstly, 30 μL of reaction mixture containing DEPC treated water, 1× DSN master buffer (50 mM Tris-HCl, pH 8.0, 5 mM $MgCl_2$ and 1 mM DTT), 0.2 mM ATP, 100 nM donor RNA, and target PNK with indicated concentration was prepared. For nuclease test, 150 U/mL RNase If was added to the reaction mixture. The mixture was incubated at 37 °C for 30 min to perform the PNK-catalyzed phosphorylation reaction, followed by inactivation at 65 °C for 20 min. Subsequently, 250 nM

Taqman probe, 100 nM acceptor RNA and 30 U/mL Rnl2 were added, and the ligation reaction was carried out at 37 °C for 60 min. Finally, 3 U/mL DSN was added to the reaction mixture, followed by incubation at 55 °C for 30 min. The 30 μL of reaction products was diluted to 60 μL with DEPC-treated water for fluorescence spectra measurement. The fluorescence spectra were measured by an F-7000 fluorescence spectrophotometer (Hitachi, Japan) equipped with a xenon lamp as the excitation source. The spectra were recorded in the range from 503 to 640 nm at an excitation wavelength of 490 nm. The excitation and emission slits were set for 5.0 nm and 5.0 nm, respectively.

DNA Assay. A volume of 30 μL reaction mixture containing DEPC treated water, 1× DSN master buffer (50 mM Tris-HCl (pH 8.0), 5 mM MgCl2 and 1 mM DTT), 0.2 mM ATP, 30 U/mL Rnl2, 100 nM RNA 1, 100 nM RNA 2 and target PNK with indicated concentration was prepared. The ligation reaction was carried out at 37 °C for 60 min, followed by inactivation at 80 °C for 5 min. Then 250 nM Taqman probe and 3 U/mL DSN were added to the reaction mixture and incubated at 55 °C for 30 min. The reaction products (30 μL) were diluted to 60 μL with DEPC treated water for the measurement of fluorescence spectra. The fluorescence spectra were measured by an F-7000 fluorescence spectrophotometer (Hitachi, Japan) equipped with a xenon lamp as the excitation source. The spectra were recorded in the range from 503 to 650 nm at an excitation wavelength of 490 nm. The excitation and emission slits were set for 5.0 and 5.0 nm, respectively.

Gel Electrophoresis Analysis. The 12% nondenaturating polyacrylamide gel electrophoresis (PAGE) analysis was carried out in 1× TBE buffer (9 mM Tris-HCl, pH 8.0, 9 mM boric acid, 0.2 mM EDTA) at a 110 V constant voltage for 40 min at room temperature. The gels were analyzed by a Bio-Rad ChemiDoc MP Imaging System (USA).

PNK Inhibition Assay. For PNK inhibition assay, we used $(NH_4)_2SO_4$ and Na_2HPO_4 as the model inhibitors. Various-concentration inhibitors were mixed with PNK and incubated for 10 min prior to the phosphorylation reaction. The PNK activity assay was performed according to the procedures described above. The relative activity (*RA*) of PNK was measured according to $RA = \frac{F_i - F_0}{F_t - F_0} \times 100\%$, where F_0 is the fluorescence intensity in the absence of PNK, F_t is the fluorescence intensity in the presence of PNK, and F_i is the fluorescence intensity in the presence of both PNK and inhibitor. The IC_{50} was evaluated on the basis of the fitting curve of *RA* against the inhibitor concentration.

Preparation of Cell Extracts. Human cervical cancer cell line (HeLa cells) and lung cancer cell line (A549 cells) were cultured in Dulbecco's modified Eagle's medium (DMEM) supplemented with 10% fetal bovine serum (FBS) and 1% penicillin-streptomycin. The cells were incubated at 37 °C in a humidified chamber with 5% CO_2. About 1×10^6 cells were collected for PNK extraction using nucleoprotein extraction kit (Shanghai Sangon, China) according to the manufacturer's handbook. The cell extracts were then diluted to prepare PNK solutions equivalent to 1 to 10000 cells, and the PNK activity is measured according to the procedures described above.

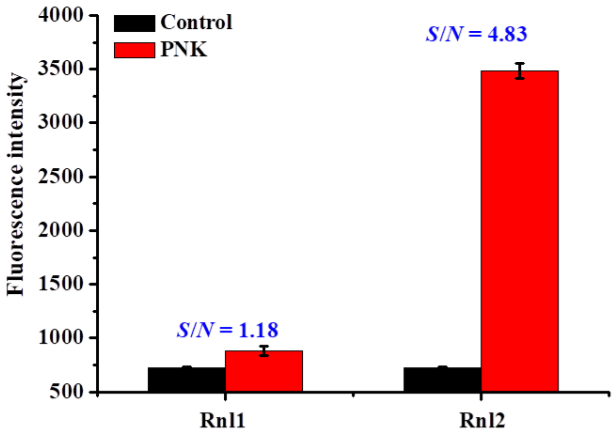

Fig. S1 Measurement of fluorescence intensity in response to 50 U/mL PNK (red column) and the control group without PNK (black column) in the presence of Rnl1 (30 U/mL) and Rnl2 (30 U/mL), respectively. S/N refers to the signal-to-noise ratio. Error bars represent the standard deviations of three independent measurements.

Comparison of T4 RNA ligase 1 and T4 RNA ligase 2 on assay performance. T4 RNA ligase 1 (Rnl1) and T4 RNA ligase 2 (Rnl2) are two main RNA ligases used for RNA ligation. We compared the assay performance using Rnl1 and Rnl2, respectively (Fig. S1). Both Rnl1 and Rnl2 generate a low background signal when PNK target is absent due to no occurrence of target-induced signal amplification. In contrast, upon the addition of PNK, an enhanced fluorescence signal is detected in both groups, with a signal-to-noise ratio (S/N) of 4.83 for Rnl2 group and 1.18 for Rnl1 group. The difference may be explained by the higher ligation rate of Rnl2 (> 10 min^{-1}) than that of Rnl1 (0.1 to 1 min^{-1}).[1] Therefore, Rnl2 is used for RNA ligation in subsequent research.

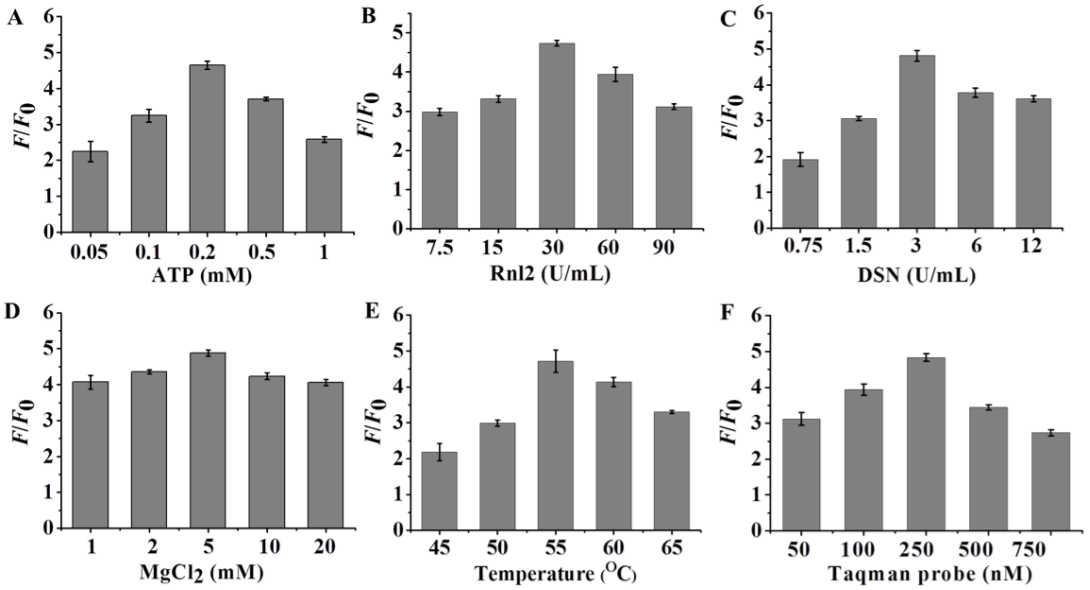

Fig. S2 Variance of the F/F_0 value with the ATP concentration (A), Rnl2 concentration (B), DSN concentration (C), $MgCl_2$ concentration (D), reaction temperature (E), and Taqman probe concentration (F). F and F_0 represent the fluorescence intensity of FAM at 520 nm in the presence and absence of PNK, respectively. The PNK concentration is 30 U/mL. Error bars represent the standard deviations of three independent experiments.

Optimization of the Experimental Conditions. To achieve the best assay performance, we optimized the experimental conditions including the concentrations of ATP, Rnl2, DSN, $MgCl_2$, Taqman probe, and the reaction temperature. We used the F/F_0 value to quantitatively evaluate the assay performance, where F is the fluorescence intensity of FAM at 520 nm in the presence of 30 U/mL PNK, and F_0 is the fluorescence intensity of FAM at 520 nm in the absence of PNK. ATP is the substrate of PNK, and it provides phosphate group for PNK-catalyzed phosphorylation of donor, and thus the concentration of ATP should be optimized. As shown in Fig. S2A, the F/F_0 value enhances with the increasing concentration of ATP from 0.05 to 0.2 mM, followed by the decrease beyond the concentration of 0.2 mM, because the excess ATP will inhibit PNK activity

through blocking the binding site of PNK protein.[2] Therefore, 0.2 mM ATP is used in the subsequent researches.

Rnl2 is a core enzyme in the proposed ligase-based amplification assay system. Large amounts of Rnl2 can promote the ligation of donor RNA with acceptor RNA to produce abundant RNA triggers (Scheme 1), but excess Rnl2 may cause intramolecular circularization of the single-stranded donor RNA through the formation of ligase-adenylate and RNA-adenylate intermediates,[3] which cannot be used for the ligation with acceptor RNA. As shown in Fig. S2B, the F/F_0 value enhances with the increasing concentration of Rnl2 from 7.5 to 30 U/mL, followed by the decrease beyond the concentration of 30 U/mL. Therefore, 30 U/mL Rnl2 is used in the subsequent researches.

The DSN enzyme is an important tool enzyme for signal amplification in this assay. High-concentration DSN benefits the cleavage of more Taqman probes, but the excess DSN may cause high background signal due to the nonspecific cleavage of single-stranded Taqman probes.[4] As shown in Fi. S2C, the F/F_0 value improves with the increasing concentration of DSN from 0.75 to 3 U/mL, followed by the decreases beyond the concentration of 3 U/mL. Therefore, 3 U/mL DSN is used in the subsequent researches.

We further investigate the effect of Mg^{2+} (the cofactor of DSN enzyme) upon the assay performance. As shown in Fig. S2D, the F/F_0 value enhances with the increasing concentration of $MgCl_2$ from 1 to 5 mM, and then levels off at the concentration of 5 mM. Therefore, 5 mM is selected as the optimal $MgCl_2$ concentration.

The high temperature can promote the DSN activity by facilitating the faster hybridization and the subsequent dissociation of RNA trigger in DNS-mediated cleavage reaction, but exorbitant

temperature may reduce DSN activity due to the heat inactivation of enzyme protein.[5] Therefore, the reaction temperature of DSN should be optimized. As shown in Fig. S2E, the F/F_0 value improves with the increase of reaction temperature from 45 to 55 ℃, followed by the decrease beyond 55 ℃. Therefore, 55 ℃ is used as the optimal reaction temperature in the subsequent researches.

Finally, we investigated the effect of Taqman probe concentration upon the assay performance. Taqman probe is used for signal output in the proposed assay. High-concentration Taqman probe is helpful for the generation of a high fluorescence signal, but excess Taqman probes may cause high background signal due to the non-complete quenching of FAM fluorescence.[4] As shown in Fig. S2F, the F/F_0 value improves with the increasing concentration of Taqman probe from 50 to 250 nM, followed by decrease beyond the concentration of 250 nM. Therefore, 250 nM Taqman probe is used in the subsequent researches.

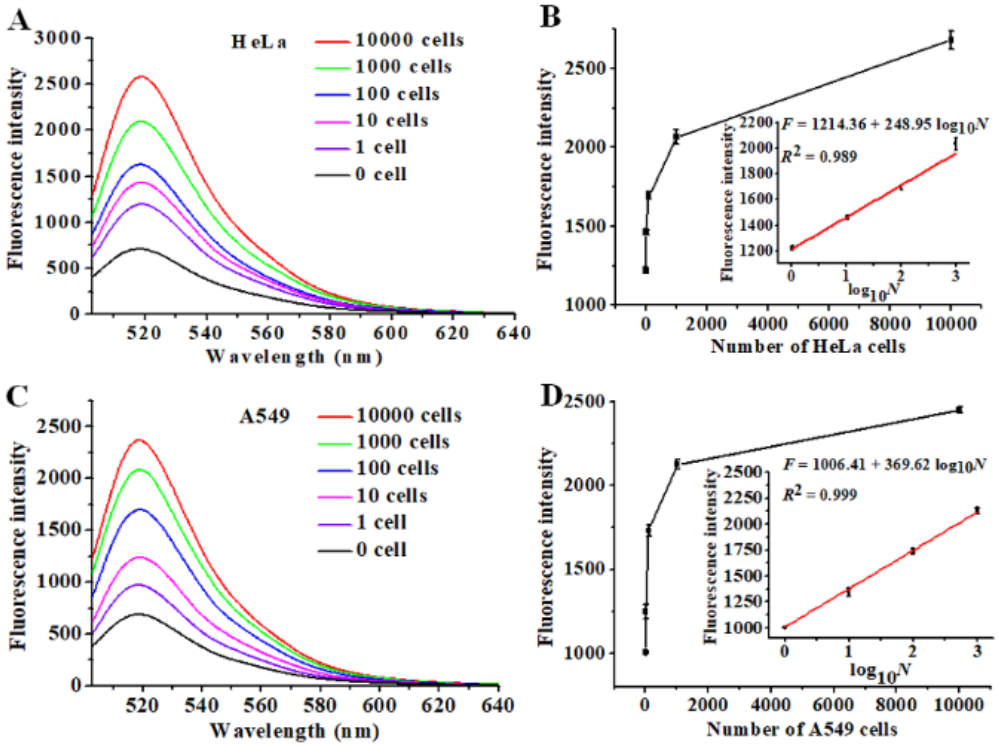

Fig. S3 (A) Measurement of fluorescence emission spectra in response to different HeLa cell number. (B) Variance of fluorescence intensity with the HeLa cell number. Inset shows the linear relationship between the fluorescence intensity and the logarithm of HeLa cell number. (C) Measurement of fluorescence emission spectra in response to different A549 cell number. (D) Variance of fluorescence intensity with A549 cell number. Inset shows the linear relationship between the fluorescence intensity and the logarithm of A549 cell number. Error bars represent the standard deviations of three independent experiments.

The deregulation of cellular PNK activity is closely associated with a variety of human diseases including cancers, and sensitive detection of endogenous PNK activity is of great importance to PNK-related biomedical researches and disease diagnosis.[6] To evaluate the feasibility of the proposed method for real sample analysis, we measured the PNK activity in human cervical cancer cell line (HeLa cells) and lung cancer cell line (A549 cells). Fig. S3A shows that the

fluorescence intensity improves with the increasing number of HeLa cells from 0 to 10000 cells. The fluorescence intensity is linearly dependent on the HeLa cell number from 1 to 1000 cells (Fig. S3B), and the corresponding equation is $F = 1214.36 + 248.95\log_{10} N$ with R^2 of 0.989, where F is the fluorescence intensity and N is the HeLa cell number. Moreover, the fluorescence intensity enhances with the increasing number of A549 cells from 1 to 10000 cells (Fig. S3C), and a liner relationship is observed between the fluorescence intensity and the logarithm of the A549 cell number from 1 to 1000 cells (Fig. S3D), with a correlation equation of $F = 1006.41 + 369.62 \log_{10} N$ ($R^2 = 0.999$), where F is the fluorescence intensity and N is the A548 cell number. Notably, the proposed method is more sensitive than the reported paper-based fluorescent assay (50 cells).[7] These results indicate that the proposed method can be used to accurately detect endogenous PNK activity with ultrahigh sensitivity.

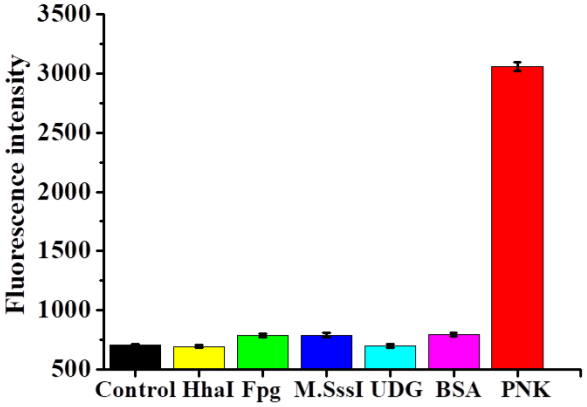

Fig. S4 Measurement of fluorescence intensity in the absence of any enzymes (control, black column) and presence of HhaI (yellow column), Fpg (green column), M.SssI (blue column), UDG (cyan column), BSA (pink column), and PNK (red column). The concentration of each enzymes is 30 U/mL, and the concentration of BSA is 10 nM. Error bars represent the standard deviations of three independent experiments.

Detection Specificity. To investigate the detection specificity of the proposed method, we used *Haemophilus haemolyticus* restriction enzyme (HhaI),[8] formamidopyrimidine [fapy]-DNA glycosylase (Fpg), CpG methyltransferase (M.SssI), uracil-DNA glycosylase (UDG), and bovine serum albumin (BSA) as the interferences. HhaI can specifically cleave the DNA strand containing the sequence of 5'-GCGC-3'. Fpg excises the damaged purine residues in the double-stranded DNA to generate the apurinic/apyrimidinic sites.[9] M.SssI methylates the cytosine residues within the sequence of 5'-CG-3'.[10] UDG can excise the uracil residues from both single- and double-stranded DNA.[11] BSA is a serum albumin protein that is commonly used as an irrelevant protein.[12] In theory, none of these interferences can induce the phosphorylation of donor RNA. Because Rnl2 is a high fidelity enzyme that can only catalyze the ligation reaction in the presence of 5' phosphorylated donor RNA,[13] no ligation reaction and subsequent cleavage reaction

can occur and thus no FAM signal can be detected. As expected, a high fluorescence signal is detected only in response to 30 U/mL PNK (Fig. S4, red column), but no distinct fluorescence signal is observed in response to HhaI (Fig. S4, yellow column), Fpg (Fig. S4, green column), M.SssI (Fig. S4, blue column), UDG (Fig. S4, cyan column), BSA (Fig. S4, pink column), and the control group without any enzyme (Fig. S4, black column). These results demonstrate the high specificity of the proposed method for PNK assay.

Table S2. Recovery Studies in 1% Fetal Bovine Serum Samples

added (U/mL)	measured (U/mL)	recovery (%)	RSD (%)
0.001	0.000973	97.3	1.63
0.01	0.0099	99	1.01
0.1	0.098	98	1.02
1	1.03	103	2.06

To investigate whether the proposed method can be applied for PNK detection in complex biological samples, we spiked various concentrations of PNK into 1% fetal bovine serum, and calculated the recoveries by using the ratio of measured concentration and added concentration. As shown in Table S2, a quantitative recovery ranging from 97.3% to 103% is obtained, suggesting the proposed method can be used for accurate PNK detection in real sample analysis.

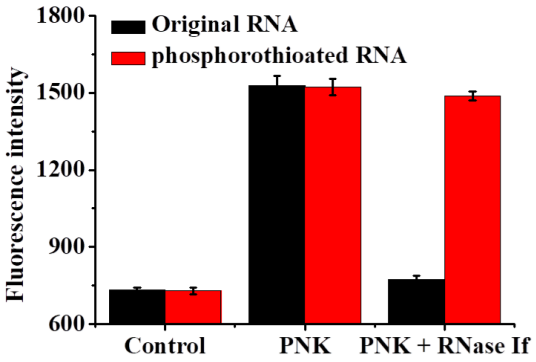

Fig. S5 Measurement of fluorescence intensity in response to the control group without PNK, 0.2 U/mL PNK, and 0.2 U/mL PNK + 150 U/mL RNase If using original RNA (black column) and phosphorothioated RNA (red column) sequences, respectively. Error bars represent the standard deviations of three independent measurements.

We further employed Ribonuclease If (RNase If) to test the influence of nuclease that will be present in clinical samples on assay performance. RNase If is an RNA endonuclease which can cleave all RNA dinucleotide bonds.[14] As shown in Fig. S5 (black column), when original RNA sequences (RNA donor and RNA acceptor) are used, the PNK treatment can generate significantly enhanced signal compared to the low background signal generated by control group without PNK, indicating PNK-induced RNA ligation and signal amplification. While with the addition of RNase If, the signal decreases down to the level of control group because RNase If may degrade all RNA donor and RNA acceptor sequences, and thus no RNA can be ligated and no signal amplification occurs. To solve this problem, we employed phosphorothioated RNA to protect the sequences from nuclease degradation. As shown in Fig. S5 (red column), when phosphorothioated RNA (RNA donor and RNA acceptor) are used, the signals of control and PNK group are similar to those of control and PNK group using original RNA (Fig. S5, black column), respectively, indicating phosphorothioate modification does not affect the ligation and signal amplification

reaction. Notably, the signal in the presence of both RNase If and PNK is similar to that of PNK treatment alone, suggesting that phosphorothioate modification of RNA sequences can protect RNA from RNase If digestion.

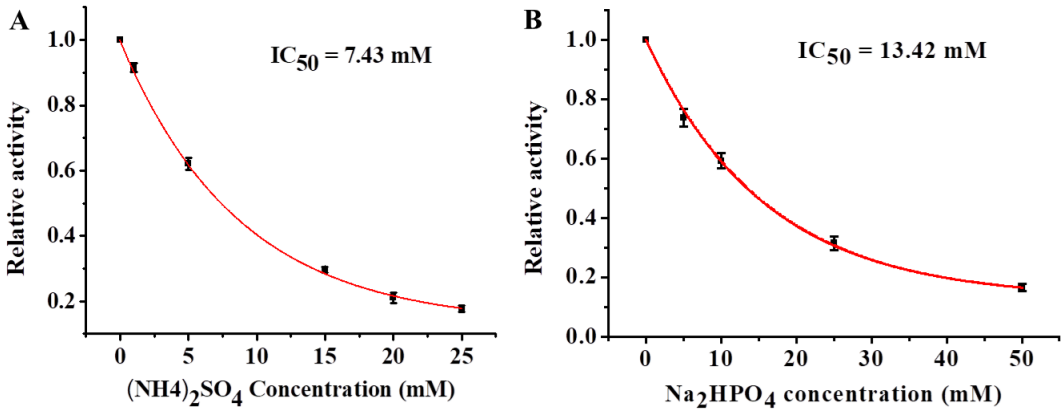

Fig. S6 Variance of relative activity of PNK with different-concentration $(NH_4)_2SO_4$ (A) and Na_2HPO_4 (B). The PNK concentration is 10 U/mL. Error bars represent the standard deviations of three independent experiments.

PNK Inhibition Assay. PNK is a potential target for disease treatment, and pharmacological inhibition of PNK activity has been regarded as a promising way for chemo- and radio-therapeutic therapy of human cancers.[15] To investigate the feasibility of the proposed method for PNK inhibition assay, we used $(NH_4)_2SO_4$ and Na_2HPO_4 as the PNK inhibitors. Both $(NH_4)_2SO_4$ and Na_2HPO_4 can efficiently inhibit PNK activity through salt-induced conformational change of PNK protein.[2] The relative activities (RA) of PNK were measured according to equation 1:

$$RA = \frac{F_i - F_0}{F_t - F_0} \times 100\% \qquad (1)$$

where F_0 is the fluorescence intensity in the absence of PNK, F_t is the fluorescence intensity in the presence of PNK, and F_i is the fluorescence intensity in the presence of both PNK and inhibitor.

As shown in Fig. S6A, the relative activity of PNK decreases with the increasing concentration of $(NH_4)_2SO_4$ from 0 to 25 mM. The half-maximal inhibitory concentration (IC_{50}) of $(NH_4)_2SO_4$ is calculated to be 7.43 mM, consistent with that obtained by bioluminescent assay (9.88 mM).[16] Moreover, the relative activity of PNK decreases with the increasing concentration of Na_2HPO_4 from 0 to 50 mM (Fig. S6B), and the IC_{50} value of Na_2HPO_4 is calculated to be 13.42 mM, consistent with that obtained by electrochemical assay (16 mM).[17] These results clearly demonstrate that the proposed method can be applied for PNK inhibition assay, holding great potential in drug discovery.

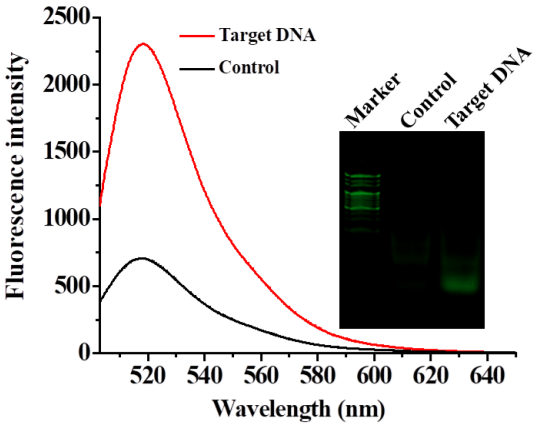

Fig. S7 Fluorescence emission spectra and PAGE analysis (insert) of the reaction in the absence (control) and in the presence of target DNA. The 100 nM target DNA, 30 U/mL ligase and 3 U/mL DSN were used in the experiments.

To demonstrate the feasibility of the proposed method for DNA assay (Scheme 2), we performed fluorescence measurements in the presence and absence of target DNA, respectively. As shown in Fig. S7, a significantly enhanced fluorescence signal is detected when target DNA is

present (Fig. S7, red curve), while no significant fluorescence signal is observed when target DNA is absent (control, Fig. S6, black curve), indicating target DNA is essential for RNA ligation and subsequent signal generation. These results are further confirmed by 12% nondenaturating polyacrylamide gel electrophoresis (PAGE) analysis. As shown in insert of Fig. S7, distinct fluorescent bands are observed when target DNA is present, indicating the target-induced cleavage of Taqman probes and the recovery of FAM fluorescence. In contrast, no band can be observed in the absence of target DNA, indicating that no cleavage reaction occurs when target DNA is absent, and consequently the Taqman probes remain intact.

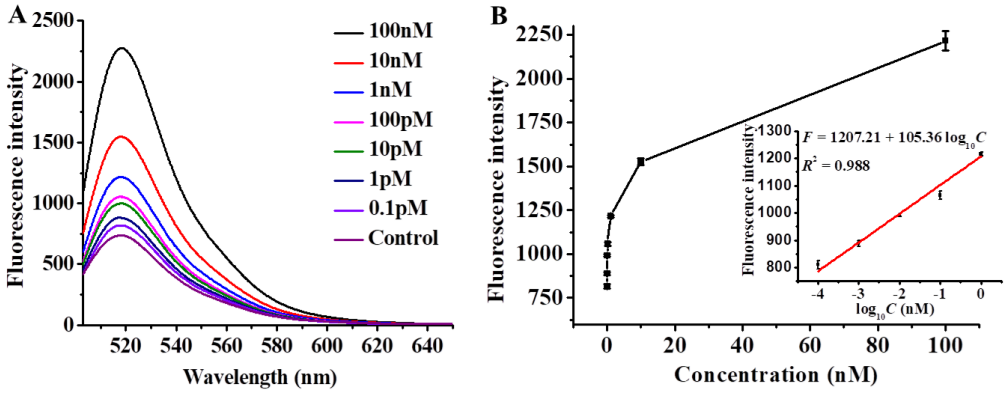

Fig. S8 (A) Fluorescence emission spectra in response to different-concentration target DNA from 0 (control) to 100 nM. (B) Variance of fluorescence intensity at 520 nm with the target DNA concentration. Inset shows the linear relationship between the fluorescence intensity and the logarithm of target DNA concentration. Error bars represent the standard deviations of three independent experiments.

We further investigated the sensitivity of the proposed method by measuring the fluorescence signals in response to different-concentration target DNA. As shown in Fig. 8A, the fluorescence

signal enhances with the increasing concentration of target DNA from 0 to 100 nM. In logarithmic scale, the fluorescence intensity exhibits a linear correlation with the target DNA concentration in the range from 0.1 pM to 1 nM with a correlation coefficient (R^2) of 0.988 (Fig. S8B). The corresponding equation is $F = 1207.21 + 105.36 \log_{10} C$, where F is the fluorescence intensity at 520 nm and C is the concentration of target DNA (nM). The detection limit is evaluated to be 0.08 pM according to the $3\sigma/K$ rule, where σ is the standard deviation of the control sample and K is the slope of the linear regression curve. The sensitivity of the proposed method is 250-fold higher than that of ligase detection reaction (LDR)-based assay (10 pM),[18] but without the involvement of any thermal cycling, providing a powerful platform for sensitive DNA detection.

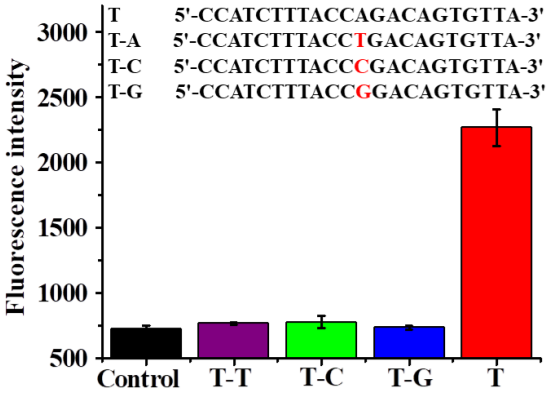

Fig. S9 Variance of fluorescence intensity in response to control samples, target DNA (T), and single-base mismatched target of T-T, T-C, and T-G, respectively. Insert shows the sequence of target DNA and single-base mismatched target, and the mutant base is shown in red color. Error bars show the standard deviation of three experiments. The 100 nM target DNA, 30 U/mL ligase and 3 U/mL DSN were used in the experiments.

To investigate the proposed assay for single nucleotide polymorphisms (SNP) detection, three

single-base mismatched target sequences are tested (Fig. S9, insert). Compared to target DNA, a middle T base of target, which is paired with 3' end base A of RNA 1, is substituted by T, C, and G in mismatched target of T-T, T-C, and T-G, respectively. Because ligation can only occur when RNA 1 matches the template perfectly, in theory, only target DNA can induce the ligation of RNA 1 and RNA 2 and subsequent the generation of fluorescence signal. As shown in Fig. S9, in comparison with the control group without any target, no enhanced signal is generated when three mismatched DNA are present, indicating no occurrence of ligation and cleavage reaction. In contrast, the signal of target DNA is 2.96, 2.92, and 3.09-fold higher than those of mismatched target of T-T, T-C, and T-G, respectively, indicating that target DNA can induce the ligation and trigger DSN-mediated signal amplification. These results clearly demonstrate the proposed method can be used for specific DNA detection and it can discriminate single-base mismatch.

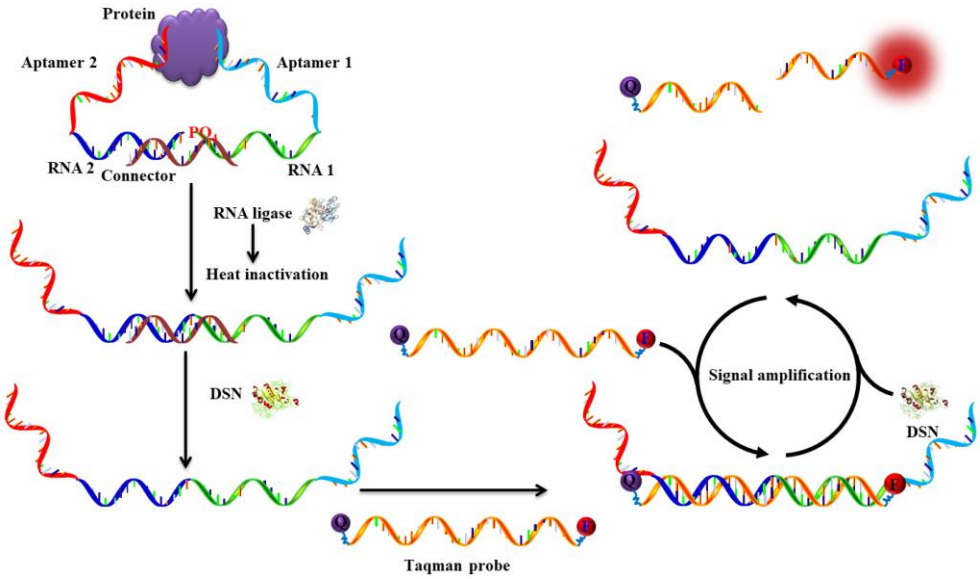

Scheme S1. Schematic illustration of the isothermal ligase-based amplification approach for protein detection.

The isothermal ligase-based amplification approach can be used for the detection of proteins and adenosine 5'-triphosphate (ATP). Sensitive detection of specific proteins is crucial for disease diagnosis, environmental monitoring, and food quality control.[19] In this research, proximity ligation strategy[20] is integrated with the isothermal ligase-based amplification approach for protein detection. As shown in Scheme S1, a pair of protein-specific aptamers (aptamer 1 and aptamer 2) are used as the ligand-binding component for specific recognition of protein target. Aptamer 1 and aptamer 2 are linked with RNA 1 and RNA 2 to form aptamer 1-RNA 1 and aptamer 2-RNA 2 oligonucleotides, respectively. The binding of aptamer 1 and aptamer 2 with protein target can bring RNA 1 and RNA 2 into proximity. By using a connector sequence as the template, the RNA 1 and RNA 2 can be ligated by RNA ligase to form a longer RNA trigger. After inactivation of ligase activity by heat treatment, DSN is added to digest the connector, and the remaining sequence containing RNA trigger will trigger the DNS-meditated signal amplification to digest

large amounts of Taqman probes, generating an amplified fluorescence signal. In contrast, in the absence of protein target, RNA 1 and RNA 2 is separated, and the connector is too short to ligate RNA 1 and RNA 2. As a result, no DNS-meditated signal amplification can be initiated and no fluorescence signal is detected.

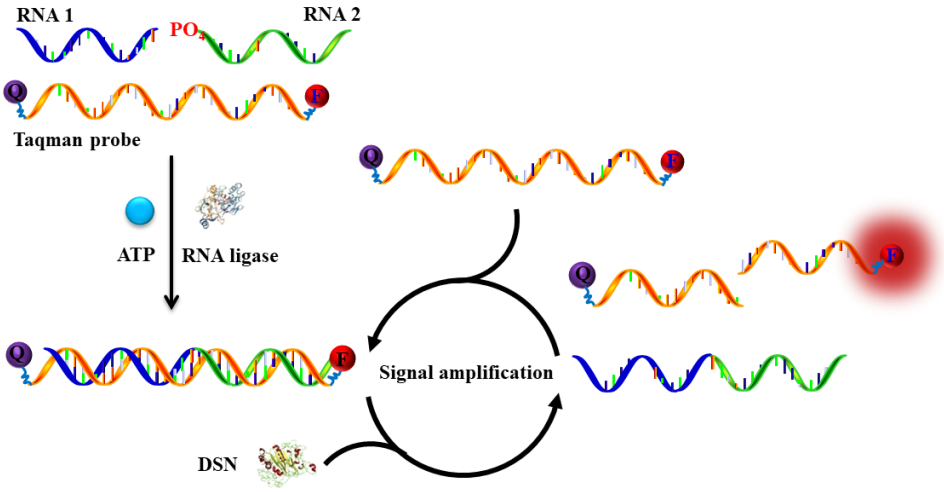

Scheme S2. Schematic illustration of the isothermal ligase-based amplification approach for ATP detection.

Adenosine 5'-triphosphate (ATP) is a universal energy storage molecule existed in all micro-organisms, and the ATP concentration is closely related to physiology and pathogenesis processes.[21] In this research, we employed the isothermal ligase-based amplification approach for ATP detection. As shown in Figure S2, two short RNA probes (RNA 1 and 5'-phosphorylated RNA 2) and a Taqman probe are employed to detect ATP. ATP is the cofactor of RNA ligase, which is essential for ligation reaction.[22] In the presence of ATP, RNA 1 and RNA 2 can be ligated by RNA ligase to form a longer RNA trigger with Taqman probe as the template. Then DSN is added to initiate the DNS-meditated signal amplification to digest large amounts of Taqman probes, generating an amplified fluorescence signal. In contrast, in the absence of ATP, the activity of RNA ligase is prohibited, and thus RNA 1 and RNA 2 cannot be ligated. As a result, no DNS-meditated signal amplification can be initiated and no fluorescence signal is detected.

Table S3. Comparison of the Proposed Method with the Reported PNK Assays.

Strategy	Assay time*	Detection limit (U/mL)	Cell analysis	References
isothermal ligation-mediated cleavage reation	~ 2 h	0.000005	Yes	this work
paper-based fluorescence assay and λ exonuclease assistance	~ 5.5 h	0.0001 U	Yes	7
catalytic assembly of bimolecular beacons and λ exonuclease cleavage	~ 4 h	0.001	No	23
Graphene Oxide and λ exonuclease cleavage	~ 6 h	0.05	No	24
EXPAR and λ exonuclease cleavage	~ 2 h	0.0002	Yes	25
ferrocene-functionalized SWCNT	over 24 h	0.01	No	26
nanochannel and λ exonuclease cleavage	~ 3.5 h	0.01	No	27
copper nanoparticle and λ exonuclease cleavage	~ 1.5 h	0.49	No	28
nicking reactions-mediated	~ 9 h	0.0000436	No	29

hyperbranched rolling circle amplification	

*Assay time includes the preparation time.

REFERENCES

1. Desmond R. Bullard and Richard P. Bowater, *Biochem. J*, 2006, **398**, 135-144.
2. Z. Tang, K. Wang, W. Tan, C. Ma, J. Li, L. Liu, Q. Guo and X. Meng, *Nucleic Acids Res.*, 2005, **33**, e97-e97.
3. K. G., K. T. and L. U.Z., *FEBS Lett.*, 1974, **46**, 271-275.
4. F. Ma, W.-j. Liu, L. Liang, B. Tang and C.-Y. Zhang, *Chem. Commun.*, 2018, **54**, 2413-2416.
5. B.-C. Yin, Y.-Q. Liu and B.-C. Ye, *J. Am. Chem. Soc.*, 2012, **134**, 5064-5067.
6. (a) I. Ahel, U. Rass, S. F. El-Khamisy, S. Katyal, P. M. Clements, P. J. McKinnon, K. W. Caldecott and S. C. West, *Nature*, 2006, **443**, 713; (b) A. Chatterjee, S. Saha, A. Chakraborty, A. Silva-Fernandes, S. M. Mandal, A. Neves-Carvalho, Y. Liu, R. K. Pandita, M. L. Hegde, P. M. Hegde, I. Boldogh, T. Ashizawa, A. H. Koeppen, T. K. Pandita, P. Maciel, P. S. Sarkar and T. K. Hazra, *PLOS Genetics*, 2015, **11**, e1004749; cJ. H. J. Hoeijmakers, *Nature*, 2001, **411**, 366.
7. H. Zhang, Z. Zhao, Z. Lei and Z. Wang, *Anal. Chem.*, 2016, **88**, 11358-11363.
8. J. E. Hixson and D. T. Vernier, *J. Lipid Res.*, 1990, **31**, 545-548.
9. S. Boiteux, T. R. O'Connor, F. Lederer, A. Gouyette and J. Laval, *J. Biol. Chem.*, 1990, **265**, 3916-3922.

10. F. Ma, W.-j. Liu, B. Tang and C.-y. Zhang, *Chem. Commun.*, 2017, **53**, 6868-6871.

11. M. C. Longo, M. S. Berninger and J. L. Hartley, *Gene*, 1990, **93**, 125-128.

12. F. Ma, Y. Yang and C.-y. Zhang, *Anal. Chem.*, 2014, **86**, 6006-6011.

13. W. Cao, *Trends Biotechnol.*, 2004, **22**, 38-44.

14. P. F. Spahr and B. R. Hollingworth, *J. Biol. Chem.*, 1961, **236**, 823-831.

15. S. L. Allinson, *Future Oncology*, 2010, **6**, 1031-1042.

16. J. Du, Q. Xu, X. Lu and C.-y. Zhang, *Anal. Chem.*, 2014, **86**, 8481-8488.

17. T. Hou, X. Wang, X. Liu, C. Pan and F. Li, *Sensors and Actuators B: Chemical*, 2014, **202**, 588-593.

18. Y. S. Huh, A. J. Lowe, A. D. Strickland, C. A. Batt and D. Erickson, *J. Am. Chem. Soc.*, 2009, **131**, 2208-2213.

19. M. J. Whitcombe, I. Chianella, L. Larcombe, S. A. Piletsky, J. Noble, R. Porter and A. Horgan, *Chem. Soc. Rev.*, 2011, **40**, 1547-1571.

20. S. Fredriksson, M. Gullberg, J. Jarvius, C. Olsson, K. Pietras, S. M. Gústafsdóttir, A. Östman and U. Landegren, *Nat. Biotechnol.*, 2002, **20**, 473.

21. J.-H. Kim, J.-H. Ahn, P. W. Barone, H. Jin, J. Zhang, D. A. Heller and M. S. Strano, *Angew. Chem.*, 2010, **122**, 1498-1501.

22. E. Ohtsuka, S. Nishikawa, M. Sugiura and M. Ikehara, *Nucleic Acids Res.*, 1976, **3**, 1613-1624.

23. T. Hou, X. Wang, X. Liu, T. Lu, S. Liu and F. Li, *Anal. Chem.*, 2014, **86**, 884-890.

24. L. Lin, Y. Liu, X. Zhao and J. Li, *Anal. Chem.*, 2011, **83**, 8396-8402.

25. M. Liu, F. Ma, Q. Zhang and C.-y. Zhang, *Chem. Commun.*, 2018, **54**, 1583-1586.

26. Y. Wang, X. He, K. Wang, X. Ni, J. Su and Z. Chen, *Biosens. Bioelectron.*, 2012, **32**, 213-218.

27. L. Lin, Y. Liu, J. Yan, X. Wang and J. Li, *Anal. Chem.*, 2013, **85**, 334-340.

28. L. Zhang, J. Zhao, H. Zhang, J. Jiang and R. Yu, *Biosens. Bioelectron.*, 2013, **44**, 6-9.

29. X. Li, X. Xu, J. Song, Q. Xue, C. Li and W. Jiang, *Biosens. Bioelectron.*, 2017, **91**, 631-636.